Three-dimensional Multiharmonic Analysis of Contact and Friction in Dovetail Joints

Damien Charleux, Fabrice Thouverez, Jean-Pierre Lombard

Three-dimensional Multiharmonic Analysis of Contact and Friction in Dovetail Joints

D. Charleux, F. Thouverez
Ecole Centrale de Lyon, Laboratoire de Tribologie et de Dynamique des Systèmes
36 avenue Guy de Collongue 69134 ECULLY FRANCE

J.P. Lombard
SNECMA Moteurs, Site de Villaroche, 77550 MOISSY CRAMAYEL FRANCE

ABSTRACT

A lagrangian alternating frequency-time method for the calculation of the harmonic response of 3D structures in contact with friction is presented. Following the ideas of Nacivet *et al.* [1], the set of nonlinear equations is solved in the frequency domain while the unilateral contact and friction laws are checked in the time domain. A large number of contact elements with both normal and tangential degrees of freedom can be taken into account. This procedure is used to study a 3D model of a turbomachinery blade with dovetail attachment. A component mode synthesis is carried out and an exact dynamic reduction is then performed in the frequency domain. Only the relative displacements of the node-to-node 3D contact elements are kept in the final set of non linear equations. The blade and the corresponding jaw are subject to a constant centrifugal force and a harmonic force. The nonlinear frequency response, the normal pressure distribution and the localization of the energy dissipation are presented and discussed.

INTRODUCTION

The dovetail attachment is a widespread solution to link blades to discs in turbine engines. Figure 2 shows a dovetail attachment between a compressor blade and a jaw. This is a critical region where high stresses and friction cause wear and can lead to crack initiation [2]. Sinclair *et al.* [3] carried out an extensive study on the 2D finite element modeling of a dovetail attachment. It was showed that high stress gradients have to be expected near the contact edges. The study also revealed that very refined meshes are necessary in order to accurately predict the peak stresses. The numerical results were used to validate the analytical formulae proposed in [4]. Papanikos *et al.* [5] modeled a 3D blade to disc attachment with or without skew angle and confronted their numerical results with a 3D photoelastic analysis. They showed that a 3D calculation is needed to accurately predict the stress concentrations. The papers [2-5] are devoted to the effects of centrifugal loads, but the aerodynamic forces applied on the blade also play an important role. Periodic fluctuations of the applied pressures are often encountered. They can for instance be generated by an upstream vane wake. The resulting vibrations may produce fretting wear on the dovetail contact surfaces [6]. The object of this paper is to study the forced response of a 3D model of a blade taking into account contact and friction in the dovetail attachment.

The excitation frequencies are multiple of the rotation speed and it is therefore easy through the Campbell diagram to see if they match some resonant frequencies of the bladed disc in the speed range of interest. If a dangerous resonance is expected, one solution is to modify the blade design so as to avoid the crossing in the Campbell diagram. Another solution is to reduce amplitude levels by using friction dampers. We will not consider friction dampers in this paper. The only region of friction dissipation is the dovetail attachment itself.

Steady-state computations with numerical integration may be very long because all the transient regime has to be calculated. Under the assumption that the response is periodic, frequency methods can be used to calculate the forced response of mechanical systems involving contact with friction. Among these, the Harmonic Balance (HB)

method is convenient only for small size problems and if few harmonics are retained. This is not the case of the Incremental Harmonic Balance (IHB) method which consists of a Newton-Raphson procedure followed by a Galerkin procedure. The reverse order is known as the Galerkin/Newton-Raphson (GNR) method. Both methods give equivalent results. The IHB method is best suited for smooth nonlinearities, but Pierre *et al.* [7] achieved an extension to the case of Coulomb friction. Cameron and Griffin [8] proposed an Alternating Frequency-Time (AFT) method where the non-linear terms are computed in the time domain using FFT and inverse FFT algorithms. AFT methods are well adapted to taking into account the non-smooth multivalued Coulomb and contact laws. A GNR/AFT method was used by Berthillier *et al.* to predict the forced response of a turbomachinery blade with friction dampers [9].

Commonly used techniques to enforce the contact and friction constraints during resolution of finite elements contact problems include the penalty method, the Lagrange multipliers method and the augmented Lagrangian techniques Many papers are devoted to their application for static analysis or transient analysis by numerical integration in the time domain (see e.g. [10]). Nacivet *et al.* [1] proposed an adaptation of the lagrangian methods to the frequency domain. In conjunction with the AFT technique they formed the Dynamic Lagrangian mixed Frequency-Time (DLFT) method. In the first section of the paper, the DLFT method is revisited. It is then used to calculate the response of a blade with dovetail attachment subject to centrifugal loads and harmonic forces.

NOMENCLATURE

Vectors are boldfaced for distinction from scalars and matrices are capitalized.

M^l, C^l, K^l	: mass, damping and stiffness matrices for body *l*.
$\boldsymbol{U}^l, \dot{\boldsymbol{U}}^l, \ddot{\boldsymbol{U}}^l$	: displacement, velocity, and acceleration vectors for body *l*.
$\boldsymbol{F}_c^l$	: vector of contact forces for body *l*.
$\boldsymbol{F}_{ex}^l$	: vector of external forces body *l*.
α^l, β^l	: coefficients of proportional damping for body *l*.
$\boldsymbol{U}_r, \boldsymbol{X}_r$	: vectors of relative displacements
$\boldsymbol{V}_r$	: relative velocity
$\boldsymbol{F}_r$	: vector of reduced external forces
Λ_r	: reduced dynamic stiffness matrix
λ	: vector of Lagrange multipliers
$\lambda_{\boldsymbol{x}}, \lambda_{\boldsymbol{u}}$	: intermediate force vectors
$\lambda_{\boldsymbol{predicted}}$	: predicted contact force
μ	: coefficient of friction
ε	: penalty coefficient
dt	*:* time step

superscripts

~	: multiharmonic vector
n	: value at time t_n
N	: normal component of a vector
T	: tangential components of a vector

PRESENTATION OF THE METHOD

General formulation

Let us consider the case of two flexible solids in contact with friction. The equations of motion obtained after discretization can be written for each body *l* as

$$M^l\ddot{\boldsymbol{U}}^l + C^l\dot{\boldsymbol{U}}^l + K^l\boldsymbol{U}^l + \boldsymbol{F}_c^l = \boldsymbol{F}_{ex}^l \quad (1)$$

M^l, C^l, K^l are mass, damping and stiffness matrices for body l. $\boldsymbol{U}^l, \dot{\boldsymbol{U}}^l, \ddot{\boldsymbol{U}}^l$ are respectively the displacement, velocity, and acceleration vectors. $\boldsymbol{F}_{ex}^l$ stands for the external forces. The vector of unknown nonlinear contact forces $\boldsymbol{F}_c^l$ includes normal and tangential components.

In order to deal with contact and friction, node-to-node contact elements are defined on the contact interface. This is a valid choice in the case of matching meshes on the contact zone and if the sliding distances remain small. Rotation of the local axes may be necessary in order to have for each contact node one degree of freedom (dof) in the contact normal direction and two dofs in the tangential plane. Assuming that the steady state motion is periodic, a Galerkin procedure is performed and the equations are formulated in terms of Fourier coefficients which form multiharmonic vectors of forces and displacements. The size of the problem can then be reduced by performing two exact reductions in the frequency domain [1] . In the first one only the degrees of freedom involved in the contact elements are retained. Further factor two reduction may be obtained by writing the problem in terms of relative displacements. The equations of motion finally take the following form :

$$\Lambda_r\tilde{\boldsymbol{U}}_{\boldsymbol{r}} + \tilde{\lambda} = \tilde{\boldsymbol{F}}_{\boldsymbol{r}} \quad (2)$$

$\tilde{\boldsymbol{U}}_{\boldsymbol{r}}, \tilde{\lambda}, \tilde{\boldsymbol{F}}_{\boldsymbol{r}}$ are the multiharmonic vectors of relative displacements, Lagrange multipliers and reduced external forces respectively. Λ_r represents the reduced dynamic stiffness matrix. The Lagrange multipliers are equal to the unknown contact forces. A non linear solver is used to determine the zero of the following function :

$$\boldsymbol{f}(\tilde{\boldsymbol{U}}_{\boldsymbol{r}}) = \Lambda_r\tilde{\boldsymbol{U}}_{\boldsymbol{r}} + \tilde{\lambda} - \tilde{\boldsymbol{F}}_{\boldsymbol{r}} \quad (3)$$

At this point, the crucial problem is to determine the contact forces $\tilde{\lambda}$ for a given $\tilde{\boldsymbol{U}}_{\boldsymbol{r}}$. $\tilde{\lambda}$ is formulated as a penalization of the equation of motion in the frequency domain:

$$\tilde{\lambda} = \tilde{\boldsymbol{F}}_{\boldsymbol{r}} - \Lambda_r\tilde{\boldsymbol{U}}_{\boldsymbol{r}} + \varepsilon(\tilde{\boldsymbol{U}}_{\boldsymbol{r}} - \tilde{\boldsymbol{X}}_{\boldsymbol{r}}) \quad (4)$$

where ε is a penalty coefficient and $\tilde{\boldsymbol{X}}_{\boldsymbol{r}}$ is a new vector of relative displacements. It will be seen in the next section that the pair $(\tilde{\boldsymbol{X}}_{\boldsymbol{r}}, \tilde{\lambda})$ is determined through an Alternating Frequency Time (AFT) method so that the contact and friction conditions are fulfilled in the time domain. Equation (3) boils down to $\boldsymbol{f}(\tilde{\boldsymbol{U}}_{\boldsymbol{r}}) = \varepsilon(\tilde{\boldsymbol{U}}_{\boldsymbol{r}} - \tilde{\boldsymbol{X}}_{\boldsymbol{r}})$. So it can be seen that the convergence ensures that (2) is verified and that contact and friction are taken into account since then $\tilde{\boldsymbol{U}}_{\boldsymbol{r}} = \tilde{\boldsymbol{X}}_{\boldsymbol{r}}$. The value of the penalty coefficient may affect the convergence and the accuracy of the solution. It should be chosen so as to balance the contributions of the equation of motion to be solved and of the contact constraints. Taking the spectral radius of the dynamic stiffness matrix $\rho(\Lambda_r)$ generally gives good results.

Computation of the contact forces in the time domain

Equation (4) can be reformulated as

$$\tilde{\lambda} = \tilde{\lambda}_{\boldsymbol{u}}(\tilde{\boldsymbol{U}}_{\boldsymbol{r}}) - \tilde{\lambda}_{\boldsymbol{x}}(\tilde{\boldsymbol{X}}_{\boldsymbol{r}}) \quad (5)$$

where

$$\tilde{\lambda}_{\boldsymbol{u}}(\tilde{\boldsymbol{U}}_{\boldsymbol{r}}) = \tilde{\boldsymbol{F}}_{\boldsymbol{r}} - \Lambda_r\tilde{\boldsymbol{U}}_{\boldsymbol{r}} + \varepsilon\tilde{\boldsymbol{U}}_{\boldsymbol{r}}, \quad \tilde{\lambda}_{\boldsymbol{x}}(\tilde{\boldsymbol{X}}_{\boldsymbol{r}}) = \varepsilon\tilde{\boldsymbol{X}}_{\boldsymbol{r}} \quad (6)$$

A given contact element is now considered. For this contact element, the counterparts of $\tilde{\lambda}, \tilde{\boldsymbol{X}}_{\boldsymbol{r}}, \tilde{\lambda}_{\boldsymbol{u}}, \tilde{\lambda}_{\boldsymbol{x}}$ in the time domain are $\{\lambda^{\boldsymbol{n}}\}_{\boldsymbol{n}=1..\boldsymbol{N}}, \{\boldsymbol{X}_{\boldsymbol{r}}^{\boldsymbol{n}}\}_{\boldsymbol{n}=1..\boldsymbol{N}}, \{\lambda_{\boldsymbol{u}}^{\boldsymbol{n}}\}_{\boldsymbol{n}=1..\boldsymbol{N}}$ and $\{\lambda_{\boldsymbol{x}}^{\boldsymbol{n}}\}_{\boldsymbol{n}=1..\boldsymbol{N}}$ respectively. At each iteration of the nonlinear solver, $\tilde{\lambda}_{\boldsymbol{u}}$ is calculated and $\{\lambda_{\boldsymbol{u}}^{\boldsymbol{n}}\}_{\boldsymbol{n}=1..\boldsymbol{N}}$ is obtained with an inverse FFT algorithm. A prediction–correction

strategy is used at each time increment t_n to compute the contact forces $\lambda^{\boldsymbol{n}}$. A predicted contact force is calculated assuming that the vector of relative tangential displacements $\boldsymbol{X}_r^{\boldsymbol{T}}$ remains the same between t_{n-1} and t_n, and that the normal relative motion X_r^N is zero. This leads to

Prediction : $\lambda_{\boldsymbol{predicted}}^{\boldsymbol{n,T}} = \lambda_{\boldsymbol{u}}^{\boldsymbol{n,T}} - \lambda_{\boldsymbol{x}}^{\boldsymbol{n-1,T}}$, $\lambda_{predicted}^{n,N} = \lambda_u^{n,N}$

The next step is to correct the contact force so that the complete contact law is verified. This is done by computing $\lambda_{\boldsymbol{x}}^{\boldsymbol{n}}$ and the corrected contact force is then given by

Correction : $\lambda^{\boldsymbol{n}} = \lambda_{\boldsymbol{u}}^{\boldsymbol{n}} - \lambda_{\boldsymbol{x}}^{\boldsymbol{n}}$

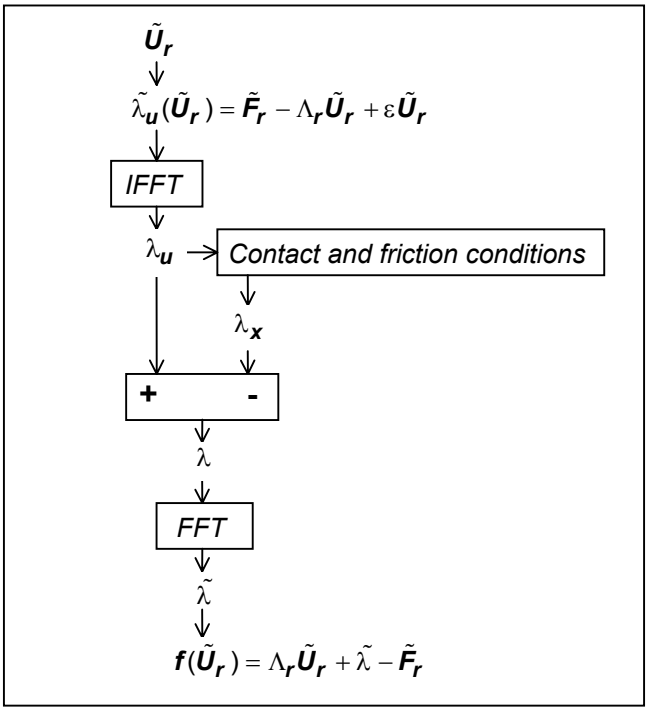

Fig 1 : implementation of the DLFT method

In order to calculate $\lambda_{\boldsymbol{x}}^{\boldsymbol{n}}$, three cases must be distinguished :

- **Separation** : $\lambda_{predicted}^{n,N} \geq 0$

  The predicted force is a traction force which means that the contact is lost. The contact force has to be set to zero which requires

$$\lambda_{\boldsymbol{x}}^{\boldsymbol{n}} = \lambda_{\boldsymbol{u}}^{\boldsymbol{n}} \tag{7}$$

- **Stick** : $\lambda_{predicted}^{n,N} < 0$ and $\left\|\lambda_{\boldsymbol{predicted}}^{\boldsymbol{n,T}}\right\| < \mu\left|\lambda_{predicted}^{n,N}\right|$

  The normal relative displacement is zero and the tangential relative displacement is constant. This leads to

$$\lambda_x^{n,N} = 0, \quad \lambda_{\boldsymbol{x}}^{\boldsymbol{n,T}} = \lambda_{\boldsymbol{x}}^{\boldsymbol{n-1,T}} \tag{8}$$

- **Slip** : $\lambda_{predicted}^{n,N} < 0$ and $\left\|\lambda_{\boldsymbol{predicted}}^{\boldsymbol{n,T}}\right\| \geq \mu\left|\lambda_{predicted}^{n,N}\right|$

Again, there is no normal relative displacement. The correction is made assuming that the normal force does not change and that the tangential contact force has and the same direction as the tangential predicted force. The tangential relative speed implicitly defined by

$$V_r^{n,T} = \frac{\lambda_x^{n,T} - \lambda_x^{n-1,T}}{\varepsilon dt} \tag{9}$$

must be in the direction of the predicted force and the contact force must be on the Coulomb cone. Therefore, λ_x^n is given by

$$\lambda_x^{n,N} = 0, \quad \lambda_x^{n,T} = \lambda_x^{n-1,T} + \lambda_{predicted}^{n,T} \left(1 - \mu \frac{\left| \lambda_{predicted}^{n,N} \right|}{\left\| \lambda_{predicted}^{n,T} \right\|} \right) \tag{10}$$

The different steps of the proposed method are summarized in the diagram of figure 1.

PRESENTATION OF THE STUDIED CASE

The two parts in contact are a compressor blade and the corresponding jaw. Figure 2 gives a view of their finite elements meshes. The jaw plays the role of a disc sector. The bottom plane of the jaw is fixed and due to the centrifugal forces applied, contact occurs on the two plane flanks of the dovetail attachment. The meshes coincide with each other in the contact region. Each flank consists of 4*9 nodes. A total of 72 node-to-node contact elements are thus defined to carry out the simulations. The flank angle is 45° and the skew angle is 25°.

The main objective here is to study the impact of the frictional damping on the forced response of the blade. The impact on aeroelastic stability is outside the scope of this paper. We aim at simulating the dynamical behavior of the blade in a frequency range around the first resonance of the blade with a particular attention to the amplitude reductions resulting from friction dissipation.

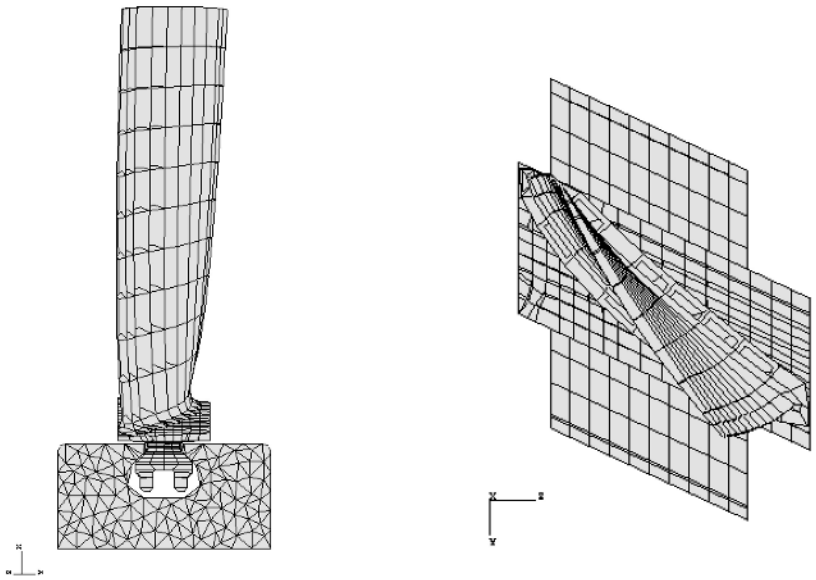

Fig 2 : views of the blade and the jaw

The Craig & Bampton component mode synthesis [11] is used on each body to reduce the number of unknowns. All the contact nodes are retained plus one node at the top of the blade to apply the harmonic excitation. The reduced basis is completed with 6 normal modes for each substructure. A centrifugal load corresponding to a rotation speed of 5 000 rpm is applied which brings about stiffness corrections. The two parts are treated

separately during this stage. The jaw does not support the load due to the blade. This is not very important since its first frequency is far beyond the frequency range that is studied. As regards the blade, the contact nodes are fixed. The static equilibrium is determined later, taking contact and friction into account with a static procedure similar to the one presented in the first section. All these preliminary calculations are performed using the commercial code SAMCEF. The mass and stiffness matrices and the vector of centrifugal loads expressed in the reduced basis are retrieved and form the inputs of our contact program. The damping matrices are derived assuming a Rayleigh damping :

$$C^l = \alpha^l K^l + \beta^l M^l \tag{11}$$

RESULTS

Static equilibrium

The friction coefficient is set to 0.3. The centrifugal loads cause all the contact elements to slide, that is to say that all the contact forces are located on the Coulomb cone. The sliding distances go up to 40μm which is less than 5% of the distance between two consecutive nodes. Thus the choice of the node-to-node treatment of contact seems valid. Figure 3 shows the spatial distribution of the normal contact forces. All the contact forces are positive which means that no separation of the contact interfaces occur. It can be seen that the pressure is not uniform. Sinclair *et al.* [3] showed that important pressure peaks should be expected near the edges of the flanks. Our results give the same trend even if our mesh is too coarse to see precisely this effect.

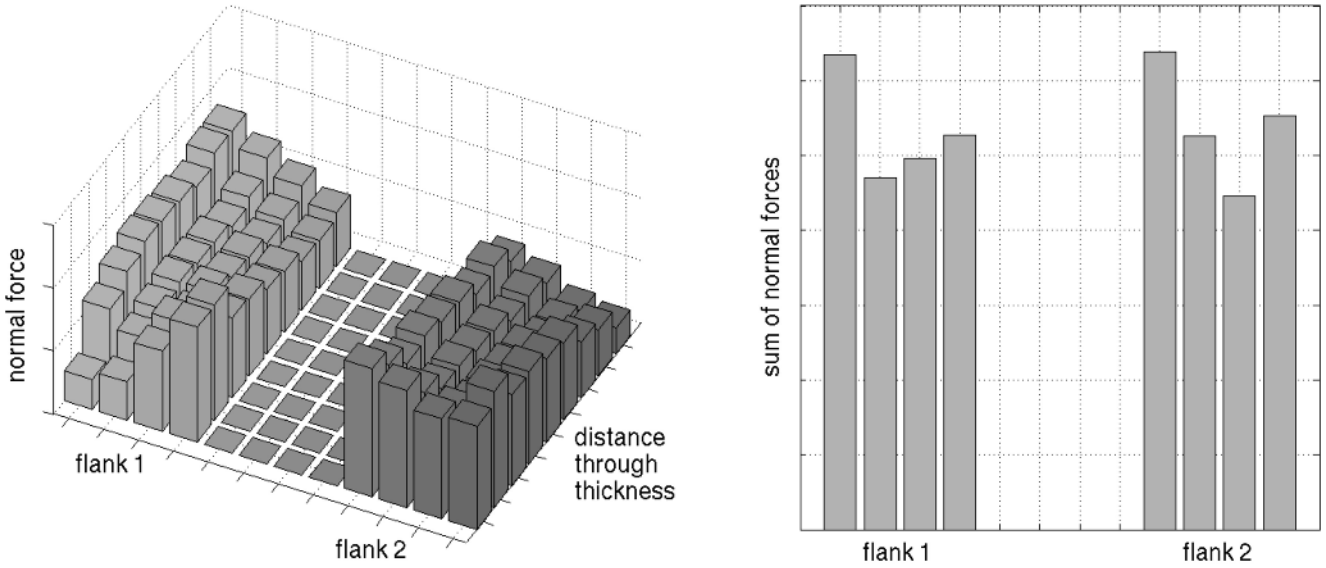

Fig 3 : (left) normal forces computed for each contact element,
(right) summation of the normal forces for each line of contact elements

Frequency response

A harmonic excitation is applied on a dof located at the top of the leading edge. Figure 4 shows the amplitudes computed for the same dof. The resonance studied here corresponds to the first bending mode of the blade. The linear curve corresponds to the case where no slip occurs and can be obtained for instance by setting the friction coefficient to a sufficiently high value. The damping coefficients α^l, β^l were chosen so as to get a damping factor equal to 0.1% on the linear curve.

A friction coefficient of 0.3 was retained for the nonlinear computations. A hybrid Powell procedure [12] is used to solve the nonlinear equations in the frequency domain. The solution obtained for a given frequency is used as a starting point for the resolution of the next frequency in order to make convergence easier. Figure 4 shows the

solutions obtained with one harmonics and three harmonics. In both cases, convergence has been achieved on all the frequency range. Far enough from the resonance frequency the amplitude is seen to be very close to that obtained in the all stuck case whereas near the resonance frequency strong amplitude reductions are predicted. In this last case, intermittent separation is also found for eight contact elements. Figure 5 shows that they are located at the bottom of the flanks. Coming back to figure 3 points out that the contact is lost where stresses caused by centrifugal forces are low.

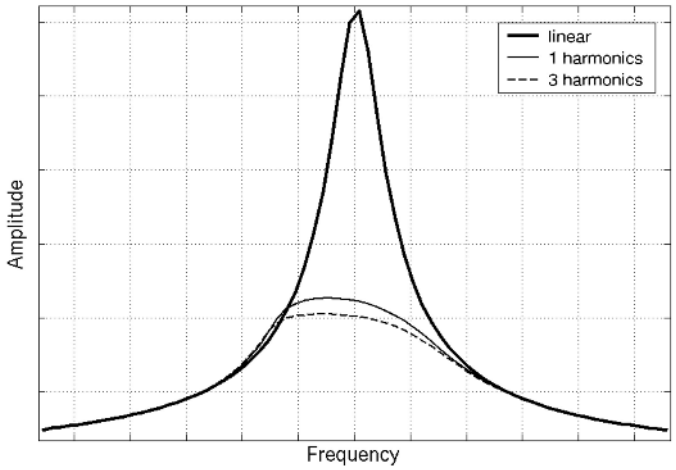

Fig 4 : Numerical frequency response for the first blade mode, displacement at tip, tangential direction (Y)

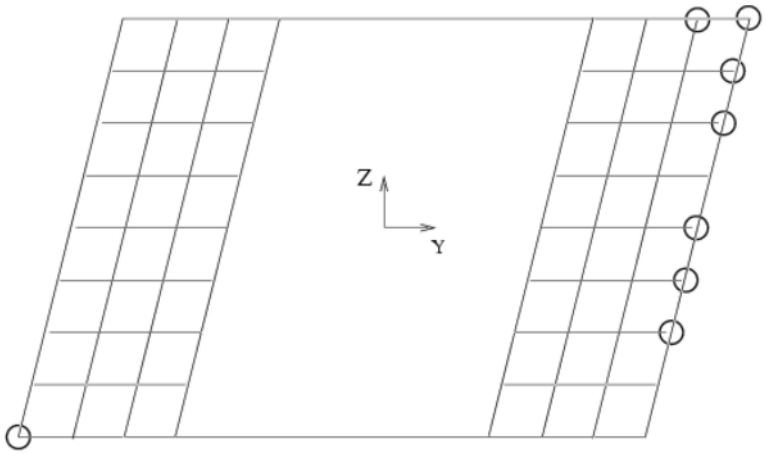

Fig 5 : localization of the nodes where separation occurs

Sliding distances are much shorter than those due to centrifugal preload. The contact interface is never altogether in a sliding status. Figure 6 provides the distribution of the energy dissipations. What is calculated exactly here is the average dissipation power, i.e. the energy dissipation per period. One can notice that the distribution is not uniform. Some points barely slide and seem to act as pivots.

Simulations featuring fewer contact elements were also conducted and greater amplitude reductions were found. It was noted that spatial convergence was not completely achieved for a model with 72 contact elements. This highlights the need for more refined grids in the contact region.

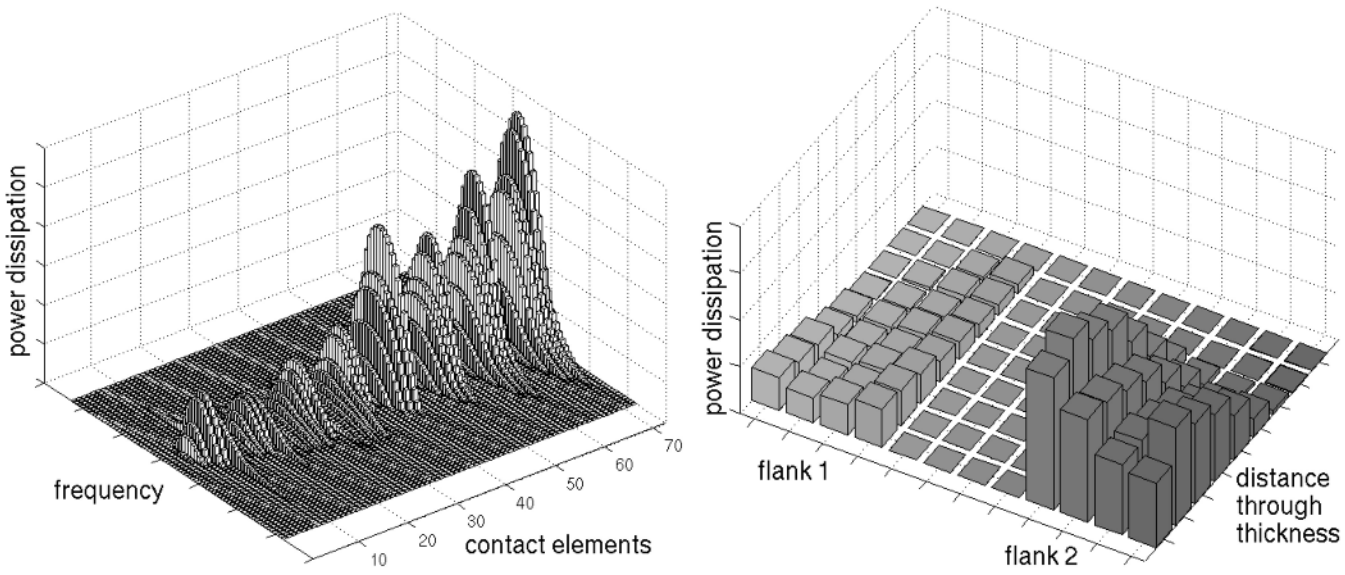

Fig 6 : (left) power dissipations - one value per contact element and per frequency, (right) distribution of the power dissipations - summation on all the frequencies.

CONCLUSIONS

The DLFT method has been revisited and used to calculate the forced response of a blade. Unilateral contact and friction on the two flats of the dovetail region have been taken into account using a total of 72 3D node-to-node contact elements. A static analysis was first performed. The results show agreement with the general trends given in [2-6]. More refined meshes are required if accurate prediction of the contact pressure distributions is desired. The harmonic response shows significant amplitude reductions near the resonant frequency. The amplitude is very close to that calculated without considering friction elsewhere. The study also reveals that partial separation of the contact surfaces occurs near the resonant frequency. Experimental validation of these last results are needed.

ACKNOWLEDGMENTS

We are pleased to acknowledge the technical and financial support of this work by SNECMA Moteurs. We are also grateful to S. Nacivet for many fruitful discussions.

REFERENCES

[1] Nacivet S., Pierre C., Thouverez F., Jezequel L., *A dynamic Lagrangian frequency-time method for the vibration of dry-friction-damped systems,* Journal of Sound and Vibration, vol 265, no 1, pp 201-219, 2003.

[2] Meguid S.A., Refaat M.H., Papanikos P., *Theoretical and experimental studies of structural integrity of dovetail joints in aeroengine discs*, Journal of Materials Processing Technology, vol 56, pp 668-677, 1996.

[3] Sinclair G.B., Cormier N.G., Griffin J.H., Meda G., *Contact stresses in dovetail attachments: finite element modeling*, Journal of Engineering for Gas Turbines and Power, vol 124, pp 182-189, 2002.

[4] Sinclair G.B., Cormier N.G., *Contact stresses in dovetail attachments: physical modeling*, Journal of Engineering for Gas Turbines and Power, vol 124, pp 325-331, 2002.

[5] Papanikos P., Meguid S.A., Stjepanovic Z., *Three-dimensional nonlinear finite element analysis of dovetail joints in aeroengine discs,* Finite Elements in Analysis and Design, vol 29, pp 173-186, 1998.

[6] Fridrici V., *Fretting d'un alliage de titane revêtu et lubrifié: application au contact aube/disque*, PhD thesis, Ecole Centrale de Lyon, 2002.

[7] Pierre C., Ferri A.A., Dowell E.H., *Multi-harmonic analysis of dry friction damped systems using an incremental harmonic balance method*. Journal of Applied Mechanics, vol 52, pp 958-964, 1985.

[8] Cameron T.M., Griffin J.H., *An alternating frequency/time domain method for calculating the steady-state response of nonlinear dynamic systems*, Journal of Applied Mechanics, vol 56, pp 149-154, 1989.
[9] Berthillier M., Dupont C., Mondal R., Barrau J.J., *Blades forced response analysis with friction dampers*, Journal of Vibration and Acoustics, vol 120, pp 468-474, 1998.
[10] Simo J.C., Laursen T.A., *An augmented Lagrangian treatment of contact problems involving friction*, Computers & Structures, vol 42, no 1, pp 97-116, 1992.
[11] Craig R.R., Bampton M.C.C., *Coupling of substructures for dynamic analysis*, AIAA Journal, vol 6, no 7, pp 1313-1319, 1968.
[12] Powell M.J.D., *A hybrid method for nonlinear equations*, in P. Rabinowitz (Ed.), Numerical methods for nonlinear equations, Gordon and Breach, London ,1969.